BMC Genomics

Research article

mtDNA depletion confers specific gene expression profiles in human cells grown in culture and in xenograft

Darren Magda[1], Philip Lecane[1], Julia Prescott[1], Patricia Thiemann[1], Xuan Ma[1], Patricia K Dranchak[2], Donna M Toleno[2], Krishna Ramaswamy[2], Kimberly D Siegmund[3] and Joseph G Hacia*[2]

Address: [1]Pharmacyclics Inc., 995 East Arques Avenue, Sunnyvale, CA, 94085, USA, [2]Department of Biochemistry and Molecular Biology, University of Southern California, 2250 Alcazar Street, IGM 240, Los Angeles, CA, 90089, USA and [3]Department of Preventive Medicine, University of Southern California, Los Angeles, CA, 90089, USA

Email: Darren Magda - dmagda@pcyc.com; Philip Lecane - plecane@pcyc.com; Julia Prescott - jprescott@pcyc.com; Patricia Thiemann - tthiemann@pcyc.com; Xuan Ma - xma@pcyc.com; Patricia K Dranchak - pdrancha@usc.edu; Donna M Toleno - toleno@usc.edu; Krishna Ramaswamy - rkrishna@usc.edu; Kimberly D Siegmund - kims@usc.edu; Joseph G Hacia* - hacia@hsc.usc.edu

* Corresponding author

Abstract

Background: Interactions between the gene products encoded by the mitochondrial and nuclear genomes play critical roles in eukaryotic cellular function. However, the effects mitochondrial DNA (mtDNA) levels have on the nuclear transcriptome have not been defined under physiological conditions. In order to address this issue, we characterized the gene expression profiles of A549 lung cancer cells and their mtDNA-depleted ρ^0 counterparts grown in culture and as tumor xenografts in immune-deficient mice.

Results: Cultured A549 ρ^0 cells were respiration-deficient and showed enhanced levels of transcripts relevant to metal homeostasis, initiation of the epithelial-mesenchymal transition, and glucuronidation pathways. Several well-established HIF-regulated transcripts showed increased or decreased abundance relative to the parental cell line. Furthermore, growth in culture versus xenograft has a significantly greater influence on expression profiles, including transcripts involved in mitochondrial structure and both aerobic and anaerobic energy metabolism. However, both *in vitro* and *in vivo*, mtDNA levels explained the majority of the variance observed in the expression of transcripts in glucuronidation, tRNA synthetase, and immune surveillance related pathways. mtDNA levels in A549 xenografts also affected the expression of genes, such as *AMACR* and *PHYH*, involved in peroxisomal lipid metabolic pathways.

Conclusion: We have identified mtDNA-dependent gene expression profiles that are shared in cultured cells and in xenografts. These profiles indicate that mtDNA-depleted cells could provide informative model systems for the testing the efficacy of select classes of therapeutics, such as anti-angiogenesis agents. Furthermore, mtDNA-depleted cells grown culture and in xenografts provide a powerful means to investigate possible relationships between mitochondrial activity and gene expression profiles in normal and pathological cells.

Background

The discovery that mammalian cells grown in the presence of inhibitors of mitochondrial DNA (mtDNA) replication and transcription can lose all or almost all their mtDNA has provided a powerful means to study interactions between the mitochondrial and nuclear genomes, reviewed in [1-4]. The human mitochondrial genome is 16,569-bp in length and encodes 12S and 16S rRNAs, 22 tRNAs, and 13 polypeptides involved in the respiratory electron transport chain and ATP synthesis. The comprehensive MitoP2 database of human mitochondrial proteins http://www.mitop.de:8080/mitop2/showhumanmask.do lists 870 human mitochondrial proteins encoded by the nuclear genome [5]. Proteomic and systems biology approaches will likely unearth additional proteins directly involved in human mitochondrial function [6]. However, fundamental questions will remain about the influences mtDNA has on the regulation of nuclear genes *in vivo*.

mtDNA-depleted ρ^0 cell lines are auxotrophic for pyruvate and uridine, and are incapable of aerobic respiration due to the lack of key respiratory chain components [7,8]. Nonetheless, mtDNA-depleted cell lines possess distorted mitochondria-like structures comprised of nuclear-encoded mitochondrial proteins [9-11] and demonstrate increased invasive behavior in culture [12-17] Furthermore, mtDNA-depleted cells can grow as tumor xenografts in immune-deficient mice in some instances [18,19], but not others [20].

Here, we generated mtDNA-depleted A549 ρ^0 lung cancer cells and validated their genetic and biochemical properties in culture and tumor xenografts. Our gene expression profiling analyses of parental A549 and A549 ρ^0 cells uncovered differential expression of transcripts relevant to immune recognition, autophagy of defective mitochondria, HIF-mediated gene regulation, the epithelial-mesenchymal transition (EMT), and elimination of lipophilic molecules. Furthermore, growth in culture versus in xenograft had a greater effect on the A549 transcriptome, especially nuclear-encoded genes important for mitochondrial function and energy metabolism, than the presence of mtDNA. Overall, mtDNA-depleted cells grown in culture and in xenograft provide complementary means to identify relationships between mitochondrial activity and cellular gene expression profiles that could serve as potential biomarkers of disease.

Methods
Cells and cell culture reagents
A549 lung cancer cells were obtained from the American Type Culture Collection. Unless otherwise indicated, all cell culture reagents were purchased from Invitrogen. mtDNA-deficient A549 ρ^0 cell cultures were prepared by serial passage of parental A549 cells for 28 population doublings in standard growth media (RPMI 1640 medium supplemented with 20 mM HEPES, 2 mM L-glutamine, 10% heat inactivated fetal bovine serum (Hyclone), 200 U/mL penicillin, and 200 µg/mL streptomycin) in the presence of ethidium bromide (100 ng/mL), sodium pyruvate (1 mM), and uridine (50 µg/mL). The glucose concentration in the standard growth media is approximately 11 mM. All subsequent experiments employing A549 and A549 ρ^0 cell cultures were conducted in the same standard growth media supplemented only with sodium pyruvate (1 mM) and uridine (50 µg/mL). Growth curves were obtained by Coulter counting. All experiments were conducted using cell culture populations and not purified clones.

Estimation of mtDNA levels
mtDNA levels in A549 or A549 ρ^0 cell cultures were estimated using the pseudogene ratioing method [21]. Briefly, total DNA (both mitochondrial and genomic) was extracted from A549 or A549 ρ^0 cell cultures using the QIAamp DNA Mini Kit (Qiagen). These served as templates for PCR amplification using primers designed to anneal either to mtDNA or a previously described DNA-embedded mtDNA pseudogene (mtDNAψ) [22]. Amplicons derived from either nuclear DNA-embedded mtDNA pseudogene or mtDNA templates are predicted to be approximately the same length, but differ in sequence. These amplicons served as templates for a nested PCR using primers designed to amplify both the mtDNA-encoded *MT-CO2* and the nuclear DNA-embedded mtDNAψ sequences. The resulting amplicons were subcloned using the StrataClone™ PCR cloning system (Stratagene). Plasmid DNA from individual colonies was prepared for sequencing using the illustra TempliPhi 100/500 DNA Amplification Kit (GE Healthcare). The resulting products were sequenced using BigDye Terminator v3.0 from Applied Biosystems diluted with halfBD (Genetix Ltd.), according to manufacturer's recommendations. We obtained sequence information from 70 colonies derived from A549 DNA templates (all showed mtDNA sequences) and 92 colonies derived from A549 ρ^0 DNA templates (all showed mtDNAψ sequences). mtDNA abundance in the original A549 or A549 ρ^0 DNA preparation was estimated based on the number of colonies showing mtDNA or mtDNAψ sequences, as previously described [21].

Oxygen consumption
Oxygen consumption rates were measured using a Clark-type electrode [23]. In brief, plateau phase cultures of A549 or A549 ρ^0 cells were treated with antimycin A (1 µg/mL) or control vehicle for 3 hours. After medium was removed, cells were washed with Hanks balanced salt solution (HBSS), and harvested using trypsin/EDTA. Cells

were resuspended in complete medium, stored on ice, and aliquots were removed for Coulter counting and viability (defined as ability to exclude propidium iodide). Prior to measurement, an aliquot of cell suspension (ca. 1×10^7 cells/mL) was incubated at 37°C for 2 minutes, and then transferred to the sealed electrode chamber of an Oxytherm apparatus (Hansatech, Norfolk, UK) to measure dissolved oxygen concentration. Background oxygen consumption by the electrode in the absence of cells was subtracted from all measurements.

Quantitative RT-PCR analysis
RNA was obtained from cultured A549 cells or harvested from tumor specimens as described [24]. Total RNA was quantified using the Ribogreen RNA quantitation kit (Molecular Probes). One-step RT-PCR assays were set up in triplicate according to manufacturer's instructions using the Taqman master mix (Applied Biosystems, Inc.) and 50 ng of total RNA as template. The amount of RNA in each well was re-quantified and used for normalizations. Gene expression assay probe sets for *β-actin*, *MT-ATP6*, and *MT-CYB* were purchased from Applied Biosystems and assays were performed on an ABI PRISM 7300 instrument according to standard protocols.

ELISA and Western blotting
Total HIF-1a protein was detected by sandwich ELISA using the DuoSet IC™ HIF-1a ELISA kit obtained from R&D Systems. Briefly, 96-well plates were coated with HIF-1a capture antibody overnight prior to blocking with 5% BSA in wash buffer. Protein lysates (50 µg protein per well prepared according to the manufacturer's instructions) were added for 2 hours, whereupon plates were washed and a biotinylated detection antibody specific for HIF-1a was added. A streptavidin-horseradish peroxidase format was used for detection. The optical density at 450 minus 570 nm was measured using a microplate reader (SpectraMax Plus). HIF-1a concentrations were calculated by linear regression using a standard curve prepared from HIF-1a standard supplied with the ELISA kit.

Western blotting was performed using antibodies against GLUT1 (aka SLC2A1, rabbit polyclonal), PGK1 (goat polyclonal), MTCO2 (mouse monoclonal), PDK1 (rabbit polyclonal), and DDIT4 (rabbit polyclonal) obtained from Santa Cruz Biotechnology, Molecular Probes, Stressgen, and Proteintech, respectively. All membranes were blotted with an anti-Hsc70 (mouse monoclonal, Santa Cruz Biotechnology) antibody to control for loading and transfer. HRP-conjugated goat anti-rabbit and goat anti-mouse secondary antibodies were from Pierce. HRP-conjugated donkey anti-goat secondary antibody was from Santa Cruz Biotechnology. HRP substrate was from Pierce. Bands were imaged and quantified in the linear range and

normalized to Hsc70, using the ChemiDoc XRS Imaging System (BioRad Laboratories, Inc.).

Gene expression profiling in cell culture
A549 or A549 ρ^0 human lung cancer cells (1×10^5 cells per T-25 flask in 7 mL complete RPMI 1640 medium) were seeded 8 days prior to RNA isolation. Each experiment was performed in triplicate. After incubation, all cultures were washed twice with HBSS supplemented with 0.5% BSA and total RNA was isolated and subjected to analysis on Human Genome U133A Arrays (Affymetrix), as described [24,25]. ArrayAssist software (Stratagene) was used to generate scaled log2 transformed gene expression scores based on the RMA algorithm and to conduct hierarchical clustering analyses, as previously described [24]. Probe sets with a > 1.5-fold differential expression (two-tailed Student's t-test $P < 0.01$ subjected to Benjamini and Hochberg correction for multiple comparisons, and > 20 unit difference in the geometric mean expression scores) in a comparison of interest are reported.

We used analysis of variance to estimate the proportion of variance explained by mtDNA status and explained by growth conditions, in the gene expression profiles from A549 ρ^0 and parental A549 cells grown in culture and in xenografts. Statistical significance is determined using the Bayes Moderated F test [26] implemented using the limma package in Bioconductor [27]. This uses an empirical Bayes approach, providing more stable inference when the number of arrays is small. *P*-values are adjusted for multiple comparisons using the Benjamini and Hochberg approach to control the false-discovery rate [28].

GeneOntology and KEGG analyses were conducted using WebGestalt software http://bioinfo.vanderbilt.edu/webgestalt/[29-31]. All scaled fluorescent intensity values and .cel files are available at the National Center for Biotechnology Information (NCBI) Gene Expression Omnibus (GEO) repository http://www.ncbi.nlm.nih.gov/geo/ under Series Accession Number GSE10957. In addition, all scaled fluorescent intensity values are available in Supplemental Table 1.

Gene expression profiling in mouse xenograft models
Animal care was in accordance with NIH and institutional guidelines. For the A549 xenograft model, 1.7 million A549 cells were injected subcutaneously/intramuscularly into the right hind flank of 6 week old CD-1 nude mice that had been irradiated with 4 Gy of total body irradiation from a ^{137}Cs radiation source one day prior to tumor implantation [32]. For the A549 ρ^0 xenograft model, 1.5 million cells were used. Tumor and body weight measurements (6 or 7 mice per group) were performed three times per week once tumors became palpable. This occurred 41 versus 9 days post-implantation in ρ^0 and parental A549

Table 1: Transcripts where 90% of the variance in gene expression is explained by mtDNA status

	Affymetrix Probe ID	Gene Symbol	Entrez GeneID	Gene Description	ρ^0 Proportion of Variance[a]	F test[b]	ρ^0 Vitro/A549 Vitro		ρ^0 Vivo/A549 Vivo	
							FC[c]	P[d]	FC[c]	P[d]
Up-regulated in ρ^0 cells	214247_s_at	DKK3	27122	dickkopf homolog 3	0.98	8.62×10^{-11}	4.4	0.0009	3.7	0.0005
	209822_s_at	VLDLR	7436	very low density lipoprotein receptor	0.98	7.05×10^{-10}	3.3	0.0057	2.7	0.0002
	210105_s_at	FYN	2534	FYN oncogene	0.97	9.85×10^{-9}	3.4	0.0082	2.7	0.0009
	221305_s_at	UGT1A8	54576	UDP glucuronosyltransferase 1 family	0.97	1.21×10^{-8}	8.3	0.0088	13.1	0.0007
	202242_at	TSPAN7	7102	tetraspanin 7	0.96	3.45×10^{-11}	9.3	0.0046	9.3	0.0005
	205119_s_at	FPR1	2357	formyl peptide receptor 1	0.96	3.82×10^{-9}	3.8	0.0045	4.8	0.0010
	208596_s_at	UGT1A10	54575	UDP glucuronosyltransferase 1 family	0.96	1.20×10^{-10}	6.2	0.0051	10.2	0.0001
	219093_at	PID1	55022	hypothetical protein FLJ20701	0.95	1.41×10^{-8}	5.4	0.0090	4.2	0.0020
	209040_s_at	PSMB8	5696	proteasome subunit	0.95	2.73×10^{-10}	3.2	0.0048	2.9	0.0003
	206094_x_at	UGT1A6	54578	UDP glucuronosyltransferase 1 family	0.95	6.79×10^{-11}	5.9	0.0041	9.7	0.0001
	219959_at	PTHLH	55034	parathyroid hormone-like hormone	0.94	2.77×10^{-9}	2.8	0.0079	3.1	0.0005
	201042_at	TGM2	7052	transglutaminase 2	0.94	1.64×10^{-6}	1.6	0.0245	1.6	0.0014
	207126_x_at	UGT1A4	54657	UDP glucuronosyltransferase 1 family	0.93	3.45×10^{-11}	6.7	0.0048	11.5	0.0000
	203113_s_at	EEF1D	1936	eukaryotic translation elongation factor	0.92	1.10×10^{-5}	1.5	0.0291	1.6	0.0042
	204802_at	RRAD	6236	Ras-related associated with diabetes	0.92	9.09×10^{-7}	2.5	0.0289	2.7	0.0044
	215125_s_at	UGT1A10	54575	UDP glucuronosyltransferase 1 family	0.92	8.62×10^{-11}	7.2	0.0045	12.7	0.0001
	213587_s_at	ATP6V0E2	155066	ATPase, H+ transporting V0 subunit e2	0.92	3.60×10^{-6}	1.7	0.0447	1.9	0.0021
	217739_s_at	PBEF1	10135	pre-B-cell colony enhancing factor 1	0.91	4.54×10^{-7}	3.8	0.0141	11.0	0.0004
	204532_x_at	UGT1A4	54657	UDP glucuronosyltransferase 1 family	0.91	3.96×10^{-10}	5.8	0.0055	10.9	0.0000
	212160_at	XPOT	11260	exportin, tRNA	0.91	1.52×10^{-5}	1.6	0.0524	1.9	0.0015
	212307_s_at	OGT	8473	GlcNAc transferase	0.91	6.52×10^{-7}	1.7	0.0273	2.4	0.0007
	203262_s_at	FAM50A	9130	family with sequence similarity 50	0.91	3.01×10^{-5}	1.5	0.0435	1.6	0.0030
	217738_at	PBEF1	10135	pre-B-cell colony enhancing factor 1	0.91	1.76×10^{-7}	4.5	0.0054	11.2	0.0007
	201462_at	SCRN1	9805	secernin 1	0.90	2.79×10^{-5}	1.4	0.0186	1.5	0.0032
	219762_s_at	RPL36	25873	ribosomal protein L36	0.90	8.04×10^{-6}	1.4	0.0073	1.7	0.0014
	212909_at	LYPD1	116372	LY6/PLAUR domain containing 1	0.90	1.04×10^{-5}	2.5	0.0069	1.7	0.0050
	215025_at	NTRK3	4916	neurotrophic tyrosine kinase, receptor	0.90	6.53×10^{-7}	2.6	0.0179	2.2	0.0048
	201474_s_at	ITGA3	3675	integrin, alpha 3	0.90	1.57×10^{-6}	1.8	0.0491	1.8	0.0018
Down-regulated in ρ^0 cells	211600_at	MT-ND5	4540	mito. encoded NADH dehydrogenase 5	0.99	4.48×10^{-14}	-73.7	0.0007	-46.9	0.0001
	205674_x_at	FXYD2	486	FXYD domain ion transport regulator 2	0.98	3.45×10^{-11}	-11.0	0.0029	-14.8	0.0004

Table 1: Transcripts where 90% of the variance in gene expression is explained by mtDNA status *(Continued)*

211203_s_at	CNTN1	1272	contactin 1	0.97	4.65×10^{-9}	-4.7	0.0009	-3.6	0.0015
204698_at	ISG20	3669	interferon stimulated exonuclease gene	0.96	3.67×10^{-8}	-3.5	0.0056	-2.9	0.0014
210065_s_at	UPK1B	7348	uroplakin 1B	0.95	4.17×10^{-8}	-4.3	0.0071	-6.2	0.0013
203108_at	GPRC5A	9052	G protein-coupled receptor	0.95	4.96×10^{-9}	-3.4	0.0048	-5.9	0.0001
207434_s_at	FXYD2	4151	FXYD domain ion transport regulator 2	0.95	2.29×10^{-11}	-9.8	0.0063	-12.9	0.0003
201065_s_at	GTF2I	2969	general transcription factor II, i	0.95	6.30×10^{-7}	-2.0	0.0109	-1.7	0.0010
210064_s_at	UPK1B	7348	uroplakin 1B	0.95	1.51×10^{-8}	-5.8	0.0081	-5.9	0.0020
222088_s_at	SLC2A3	6515	solute carrier family 2, member 3	0.95	1.46×10^{-8}	-2.1	0.0080	-2.4	0.0010
33304_at	ISG20	3669	interferon stimulated exonuclease gene	0.95	3.70×10^{-7}	-2.9	0.0077	-2.4	0.0036
218995_s_at	EDN1	1906	endothelin 1	0.94	3.16×10^{-7}	-2.2	0.0333	-2.7	0.0014
219045_at	RHOF	54509	ras homolog gene family, member F	0.93	4.81×10^{-7}	-2.9	0.0062	-2.0	0.0018
214774_x_at	TNRC9	27324	trinucleotide repeat containing 9	0.93	4.39×10^{-7}	-2.9	0.0109	-3.9	0.0027
206291_at	NTS	4922	neurotensin	0.93	6.81×10^{-8}	-102	0.0009	-17.9	0.0011
201909_at	RPS4Y1	6192	ribosomal protein S4, Y-linked 1	0.92	3.55×10^{-8}	-5.8	0.0071	-18.8	0.0000
206700_s_at	JARID1D	8284	jumonji, AT rich interactive domain 1D	0.90	2.41×10^{-7}	-2.3	0.0366	-4.0	0.0000
203043_at	ZBED1	9189	zinc finger, BED-type containing 1	0.90	6.01×10^{-6}	-1.7	0.0427	-1.9	0.0026
202499_s_at	SLC2A3	6515	solute carrier family 2, member 3	0.90	2.86×10^{-6}	-1.9	0.0128	-2.3	0.0073
216623_x_at	TNRC9	27324	trinucleotide repeat containing 9	0.90	5.79×10^{-7}	-2.6	0.0128	-3.5	0.0038

[a]Proportion of variance in gene expression due to mtDNA status in cultured cells and xenografts
[b]Bayes modified F test (multiple hypothesis corrected)
[c]Fold-change
[d]Benjamini and Hochberg corrected two-tailed Student's t-test

xenograft models, respectively. Tumor volume was calculated using the equation V (mm³) = a × b²/2, where a is the largest diameter and b is the smallest diameter. No significant body weight loss was observed. To perform gene expression profiling, tumors (4 tumors per group) were harvested and snap frozen immediately on dry ice when the tumor size reached 500–800 mm³. Tumor tissue was dissected, homogenized in Trizol, and total RNA was isolated and subjected to gene expression analysis as described above.

Additional Files
Additional information about the data reported in this manuscript, including formatted gene expression data in these studies are available at *BMC Genomics*.

Results and discussion
Establishment of A549 ρ⁰ cell cultures
Candidate A549 ρ⁰ lung cancer cell cultures were prepared using previously described ethidium bromide-based protocols [12]. Consistent with prior reports of ρ⁰ cell lines (e.g. [7,9,33]), the resulting cells displayed auxotrophic growth dependence on pyruvate and uridine and elongated shape (data not shown). The growth rate of the candidate ρ⁰ cells (27 hour generation time) was slower than the parental line (20 hour generation time) in pyruvate and uridine supplemented medium (Fig. 1A).

We used the recently described pseudo-gene ratioing technique to estimate the amount of mtDNA remaining in the candidate A549 ρ⁰ cell cultures (Methods) [21]. This technique is based on quantifying the relative co-amplification of a mtDNA sequence and a nuclear-embedded mitochondrial pseudogene (mtDNAψ) sequence [22] using total DNA extracted from candidate A549 ρ⁰ cells and parental A549 cells. Assuming the mtDNAψ sequence is present in two copies per candidate A549 ρ⁰ cell, we could estimate with 95% confidence that the candidate A549 ρ⁰ cell cultures contained less than one copy of mtDNA per 14 cells. As a positive control, we used the same technique to estimate that a minimum of 45 mtDNA copies were extracted from each parental A549 cell (exact binomial upper 95% confidence limit). As a consequence of these observations, as well other biochemical characterizations described below, we will hereafter refer to the candidate A549 ρ⁰ cell cultures as A549 ρ⁰cells.

Cultured A549 ρ⁰ cells have impaired rates of oxygen consumption
To characterize mitochondrial function in the parental A549 and A549 ρ⁰ cells, we compared their rates of oxygen consumption. As expected, parental A549 cells showed robust oxygen consumption while the oxygen consumption of the A549 ρ⁰ cells was indistinguishable ($P = 0.41$)

from background (Fig. 1B). To demonstrate the involvement of respiration, we also treated parental A549 and A549 ρ⁰ cells with antimycin A, an inhibitor of mitochondrial complex III of the electron transport chain (ETC) [34], prior to measuring oxygen consumption. As expected, antimycin A-treated A549 cells showed reduced oxygen consumption, while A549 ρ⁰ cells were not significantly affected by drug-treatment (Fig. 1B). These results strongly suggest that residual mitochondria-dependent aerobic respiration in A549 ρ⁰ cells, if present, is below the threshold that can be measured in this assay.

A549 ρ⁰ cells grow in tumor xenografts at a slower rate than their parental cells
Parental A549 cells and their ρ⁰ derivatives both grew as xenografts when implanted shallowly (subcutaneously/intramuscularly) in the flank muscle of nude mice. mtDNA-depleted cell lines have been reported to form xenograft tumors [13,18,19]. Here, we found that A549 ρ⁰ cells grow readily in xenograft, although at a slower rate and after a longer induction period (approximately 30 days) relative to the parental line (Fig. 2). This is consistent with the growth characteristics of tumor xenografts derived from N2B ρ⁰ osteosarcoma [18], E3 ρ⁰ serous ovarian carcinoma [18], HSA ρ⁰ cervical cancer [18], and T47D ρ⁰ breast cancer [19] cell lines relative to their parental counterparts.

A549 ρ⁰ cells do not express mtDNA-derived transcripts in culture or in xenografts
We performed quantitative PCR analysis of mtDNA-encoded *MT-ATP6* and *MT-CYB* transcripts in A549 and A549 ρ⁰ cells grown in culture and in xenografts, in the absence of ethidium bromide. In contrast to the parental A549 cells, the expression of these two transcripts could not be detected in ρ⁰ cells (Additional File 1). This strongly suggests that, in bulk, the A549 ρ⁰ cells retained their mtDNA-depleted genotype over the course of their growth in culture and in xenograft. This was important to ascertain since it was possible that during their growth in xenograft, rare mtDNA-positive cells present in the injected A549 ρ⁰ cell population could have substantially increased in abundance and affected our downstream analyses. Similarly, it is possible that A549 or A549 ρ⁰ cells with certain genetic or epigenetic changes (e.g. those that confer a growth advantage) were selected for in culture or in xenografts and affected our results. This should be considered when interpreting the molecular analyses discussed below.

Gene expression profiling of cultured cells
Gene expression profiles were generated in plateau phase A549 and A549 ρ⁰ cells cultured in fresh medium supplemented with pyruvate and uridine prior to RNA isolation (see Additional File 2 for all data and Additional File 3 for
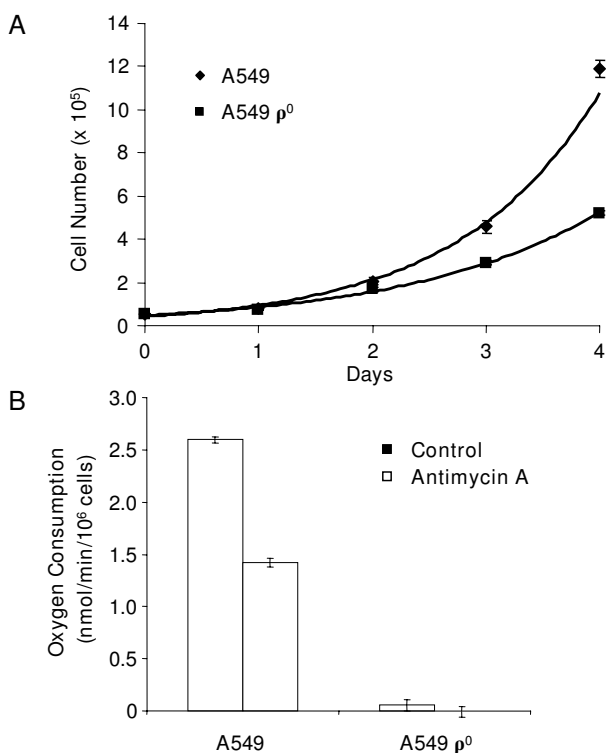
A

B

Figure 1
Characterization of cultured A549 and A549 ρ⁰ cells.
(*A*) Growth rates of A549 and A549 ρ⁰ cells in culture are
provided. Experiments were run in triplicate with error bars
representing ± 1 standard deviation. Doubling times obtained
from the fitted curves (N = $N_0 e^{rt}$) were 20.4 and 27.3 hours
for parental A549 and A549 ρ⁰ cultures, respectively. (*B*) The
oxygen consumption of A549 and A549 ρ⁰ cultured cells is
provided. Where indicated, cells were treated with 1 μg/mL
antimycin A, an inhibitor of the mitochondrial electron trans-
port chain (ETC). Experiments were run in triplicate with
error bars representing ± 1 standard deviation.

volcano plot). All 276 transcripts that were differentially
expressed (defined for every pair-wise comparison dis-
cussed hereafter as being > 1.5-fold change, two-tailed
Student's t-test *P* < 0.01 (subjected to Benjamini and
Hochberg correction for multiple comparisons), and > 20
unit difference in geometric mean expression scores) are
listed in Additional File 4. These include 131 transcripts
that were more highly expressed in A549 ρ⁰ cells and 145
that were more highly expressed in A549 cells.

Increased levels of EMT-related transcripts in cultured A549 ρ⁰ cells

To analyze differentially expressed genes in A549 cells and
their mtDNA-depleted ρ⁰ counterparts, we conducted

Gene Ontology (GO) analyses on transcripts that were
more highly expressed in the A549 ρ⁰ cells than the paren-
tal cell line (see Additional File 5A for transcript names
and Additional File 2 for data analysis of specific tran-
script). We used stringent criteria (Fisher's exact test *P* <
0.001 and at least 4 transcripts) for selection of enriched
categories. The enriched categories included those related
to cell adhesion (15 transcripts) and cell motility (4 tran-
scripts). Upon further inspection of the transcripts in
these categories, it became apparent that they reflect tran-
scriptional signatures of the epithelial-mesenchymal tran-
sition (EMT), a developmental process by which
stationary epithelial cells transform into mobile mesen-
chymal cells [35]. EMT can be driven by the activity of the
transcription factor *SNAI2*, positively regulated by *LOXL2*
[36], which leads to the over-expression of *CDH2*, *ITGB3*,
and *VIM*. All five genes are over-expressed in the ρ⁰ cells.
The fact that *CDH1* and *FGA* are also less abundant in the
ρ⁰ cells further supports the hypothesis that the ρ⁰ cells
show an increasingly mesenchymal phenotype relative to
their parental counterparts [35]. The above observations
are consistent with prior reports of mtDNA-depleted A549
cells showing increased invasive behavior relative to
parental A549 cells in a Matrigel basement membrane
matrix invasion assay system [12].

Increased metal ion binding and glucuronidation gene expression in A549 ρ⁰ cell cultures

Two enriched GO categories were related to metal ion
binding (*LOXL2* and metallothionein family members
MT1H, *MT1G*, *MT1X*, and *MT2A*) and glucuronidation
(including UDP glucuronosyltransferase 1 family mem-
bers). The increased expression of MTF-1 regulated genes
(i.e. metallothioneins) could indicate higher baseline lev-
els of oxidative stress and/or free metals in the ρ⁰ cells rel-
ative to their parental counterparts [25]. However, it is
noteworthy that several oxidative stress response genes
(e.g. *GPX2*, *GPX3*, and *GLRX*) are under-expressed in these
ρ⁰ cells. Glucuronidation is a cellular metabolic pathway
in which UDP-glucuronosyltransferases (UGTs) convert
lipophilic compounds, both endogenous and xenobiotic,
into more readily excreted polar products. UGTs catalyze
the transfer of the glucuronate moiety of uridine diphos-
phoglucuronate (UDPGA) to specific substrates, in order
to attain this increased polarity. The observed differen-
tially expressed UGT1A family members have different
substrate specificities and collectively can react with a vari-
ety of endogenous lipophilic molecules, such as fatty
acids and steroids [37-41]. Given that ρ⁰ skin fibroblasts
have impaired mitochondrial fatty acid β-oxidation [42],
we propose that the increased abundance of glucuronida-
tion-related transcripts in A549 ρ⁰ cells is a survival mech-
anism to remove excess fatty acids that are normally
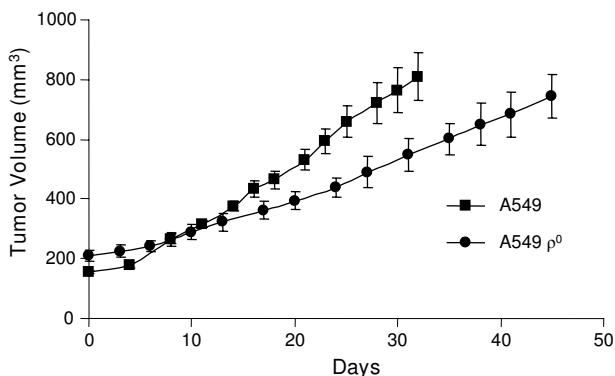metabolized to carbon dioxide and water in functional
mitochondria.

Figure 2
Growth rates of A549 and A549 ρ⁰ xenografts. Median tumor volume over time in nude mice bearing tumors derived from A549 or A549 ρ⁰ cells. Tumor volume measurements commenced at an initial average tumor volume of 155 mm³ and 208 mm³, respectively. Experiments were conducted using six or seven mice per cohort with error bars representing ± 1 standard error of the mean (SEM).

Expression profiles of HIF-1 responsive transcripts in A549 ρ⁰ cells

Next, we focused on identifying key transcription factors that could account for a significant number of over-expressed transcripts in A549 ρ⁰cells. mtDNA-deficient cells have proven useful for dissecting the role that mitochondria play in HIF-mediated responses to oxygen levels (reviewed by [43]). In fact, increased baseline levels of HIF-1 activity in cultured ρ⁰ cell lines have been noted by others [44,45]. In our A549 ρ⁰ cells, HIF-1 appeared to be an excellent candidate given the over-expression of two well-established downstream genes (*VEGFA* and *BNIP3*). We began our analyses by focusing on a group of 95 probe sets representing 63 unique HIF-1 responsive genes highlighted in a recent comprehensive review [46] (Additional File 6). While no other HIF-1 responsive genes reached our statistical criteria for over-expression, four other well-established HIF-1 regulated transcripts (*IGFBP1*, *IGFBP3*, *TF*, and *PTGS2*) were less abundant in the ρ⁰ cells relative to their parental cells. This could reflect the influence of other transcription factors or accessory proteins that regulate HIF-1 activity.

The mechanism underlying the differential expression of HIF-regulated transcripts in mtDNA-deficient cells is unknown. For example, it has been proposed that a feedback loop involving mitochondrial enzymes and citric acid cycle intermediates leads to HIF-1 stabilization and tumorigenesis in several inherited forms of cancer caused by mtDNA mutations [47]. Another possible explanation might involve insulin-like growth factor signaling which

has been shown to increase HIF-1 levels [48]. Importantly, the GO category insulin-like growth factor binding (*CYR61*, *HTRA1* aka *PRSS11*, *IGFBP4*, and *IGFBP7*) was enriched for transcripts that were more abundant in the ρ⁰ relative to parental cells (Additional File 5A).

A549 ρ⁰ cells over-express HIF-1 a protein relative to the parental cell line

To explore the mechanistic basis for the observed differential expression of HIF-responsive transcripts in culture, we measured the levels of HIF-1α protein in ρ⁰ and parental cells by ELISA (Fig. 3A). The background levels of HIF-1α were found to be 3-fold higher in ρ⁰ cells compared to the parental line. HIF-1α levels increased in the parental A549 line following treatment with cobalt acetate or incubation under hypoxic (1.5% O_2) conditions. In A549 ρ⁰ cells, HIF-1α levels were increased modestly following cobalt treatment but did not appear to be changed by hypoxic treatment. However, the level of HIF-1α protein does not solely determine its ability to induce gene expression, as post-transcriptional modifications are also known to modulate its activity [49].

To further explore the possible functional consequences of HIF-1 over-expression, we measured the levels of several HIF-regulated gene products by Western blot (Fig. 3B). The MT-CO2 product was included in this analysis to demonstrate the absence of this mtDNA-encoded protein in A549 ρ⁰ cells. In accordance with the expression data, we found that PGK1 and DDIT4 protein levels were increased in A549 ρ⁰ cells (Fig. 3B). However, GLUT1 (aka SLC2A1) protein levels were essentially unchanged in A549 and A549 ρ⁰ cells despite the fact that its transcript was 2.0-fold more abundant (corrected P = 0.017) in A549 ρ⁰ cells. As could be expected, the incubation of either parental or ρ⁰ cells in the presence of cobalt or under hypoxic conditions led to increased levels of these HIF-regulated proteins. The effect of cobalt was not as significant as that of hypoxia under these conditions. These data demonstrate that although baseline HIF-1 activity is higher in ρ⁰ than parental cells, HIF-regulated activity can be induced further in both cases.

Decreased icosanoid metabolism and cytoskeleton gene expression in cultured A549 ρ⁰ cells

In parallel, we conducted separate GO analyses on transcripts that were less abundant in A549 ρ⁰ cells ($P < 0.001$ and at least four probes sets) (Additional File 5B). The blood pressure regulation (*FGB*, *PTGS2*, *FGG*, and *FGA*) and icosanoid metabolism (*AKR1C2*, *PLA2G4A*, *PTGS2*, and *MGST2*) GO categories were significantly enriched for such transcripts. The presence of multiple fibrinogen family members in the former category could reflect possible differences in cell adhesion in ρ⁰ cells. The icosanoid metabolism category could relate to the role arachidonic

acid plays in the regulation of steroidogenesis and mitochondrial membrane permeability. It has been proposed that ATP generated by oxidative phosphorylation plays a key role in the generation and export of arachidonic acid from the mitochondria [50]. Through its role in leukotriene metabolism, arachidonic acid mediates the activity of steroidogenic acute regulatory protein (StAR), a key regulator of steroidogenesis. In addition, arachidonic acid can uncouple oxidative phosphorylation and alter mitochondrial membrane permeability [51].

The intermediate filament GO category was enriched for transcripts that were less abundant in ρ0 cells (i.e. *KRT8*, *KRT19*, *NEFL*, *KRT18*, and *DSP*). *KRT18* plays a key role in maintaining the normal morphology of mitochondria [52]. Interestingly, *VIM*, another component of intermediate filaments shown to support mitochondrial morphology and organization [53], is over-expressed in ρ0 cells. The dysregulation of intermediate filament genes in ρ0 cells could contribute to their aberrant mitochondrial morphology and/or represent cellular responses to rescue mitochondrial organization.

Increased tRNA synthetase, MHC Class I, and lysosome gene expression in A549 *ρ0* xenografts

Total RNA from A549 or A549 ρ0 tumors (four per cohort) were also subject to gene expression profiling analysis (see Additional File 3 for volcano plot). All 948 transcripts that were differentially expressed are listed in Additional File 7. These include 485 transcripts that were more highly expressed in the A549 ρ0 tumors and 463 that were more highly expressed in A549 tumors. Three major functional categories emerged from GO analyses of over-expressed genes in ρ0 xenografts (Additional File 8A). These categories were related to tRNA aminoacylation (composed of 9 tRNA synthetases), MHC class I (*B2M*, *MR1*, and six HLA gene family members), and the lysosome (23 transcripts).

The transcriptional induction of tRNA synthetases was previously highlighted in the analysis of cultured ρ0 and parental lymphoblasts [44]. Recently, there is increased evidence that tRNA synthetases have functions additional to joining specific amino acids to their cognate tRNAs. These include the regulation of angiogenesis and inflammation [54,55].

The over-expression of MHC Class I peptides is consistent with a report that MHC I is over-expressed in fibroblasts from patients with mtDNA defects as well as in cultured osteosarcoma ρ0 cells relative to their parental counterparts [56]. In that study, IFN-γ treatment enhanced MHC1 over-expression in cultured osteosarcoma ρ0 cells. Thus, the over-expression of interferon gamma receptor 1 (*INFGR1*) we observed in A549 ρ0 xenografts (1.8-fold,

corrected *P* = 0.004) could play a role in further stimulating MHC Class I peptide expression in these cells.

It has been proposed that MHC Class I over-expression in cells with mutated mitochondrial proteins provides a mechanism by which the immune system can recognize and eliminate defective cells [56]. Although ρ0 cells do not have dysfunctional proteins encoded by mtDNA, the over-expression of MHC Class I genes may simply reflect a mechanism for marking cells with defective mitochondrial function.

The over-expression of lysosome genes could relate to their function in removing defective mitochondria within cells through autophagy [57]. This could complement the immune surveillance mediated removal of cells with defective mitochondria discussed above. We speculate that the over-expression of lysosome-related genes could reflect increased numbers of lysosomes and/or simply the increased functional activity of existing lysosomes.

A549 *ρ0* xenograft transcriptomes indicate decreased cell proliferation and glycolysis

Mitosis (21 transcripts) and spindle organization and biogenesis (9 transcripts) were two major functional categories showing enrichment for down-regulated transcripts in A549 ρ0 xenografts (Additional File 8B). This would be expected given the lower proliferation rate of the A549 ρ0 cells relative to their parental counterparts (Fig. 1A). The enrichment in the actin binding (21 transcripts) and cytoskeleton protein binding (27 transcripts) categories could also reflect differences in growth rates. Alternatively, they could relate to altered mitochondrial morphology, as discussed in our analysis of cultured ρ0 cells.

Surprisingly, A549 ρ0 xenografts showed decreased expression in the glycolysis category (nine transcripts). This would appear to be counter-intuitive given the fact that these xenografts do not express mtDNA-derived transcripts (Additional File 1) or MT-COX2 protein (Fig. 3B) and thus should have severely impaired oxidative phosphorylation. Indeed, the 4.7-fold increased abundance of *PCK2* in A549 ρ0cells could indicate higher levels of gluconeogenesis, consistent with prior reports in mtDNA-depleted A549 [12], 206B ρ0osteosarcoma [58], and ARPE19 ρ0 retinal pigment epithelial [58] cultured cells. Apart from the aforementioned lower growth rate of ρ0 xenografts, this probably reflects the general reduced abundance of HIF-regulated transcripts (*GAPDH*, *PKM2*, *ENO2*, *LDHA*, *EGLN1*, *SLC2A1*, *TF*, *P4HA1*, *IGF2*, *CA9*, *HIG2*, *ADM*, and *EGLN3*) as compared to the parental A549 xenografts (Additional File 6). This occurs despite the fact that HIF-1α is over-expressed (2.6-fold, *P* = 1.6 × 10^{-4}) along with two other well-established HIF targets (*HK1* and *BHLHB3*). As discussed earlier, this is consistent
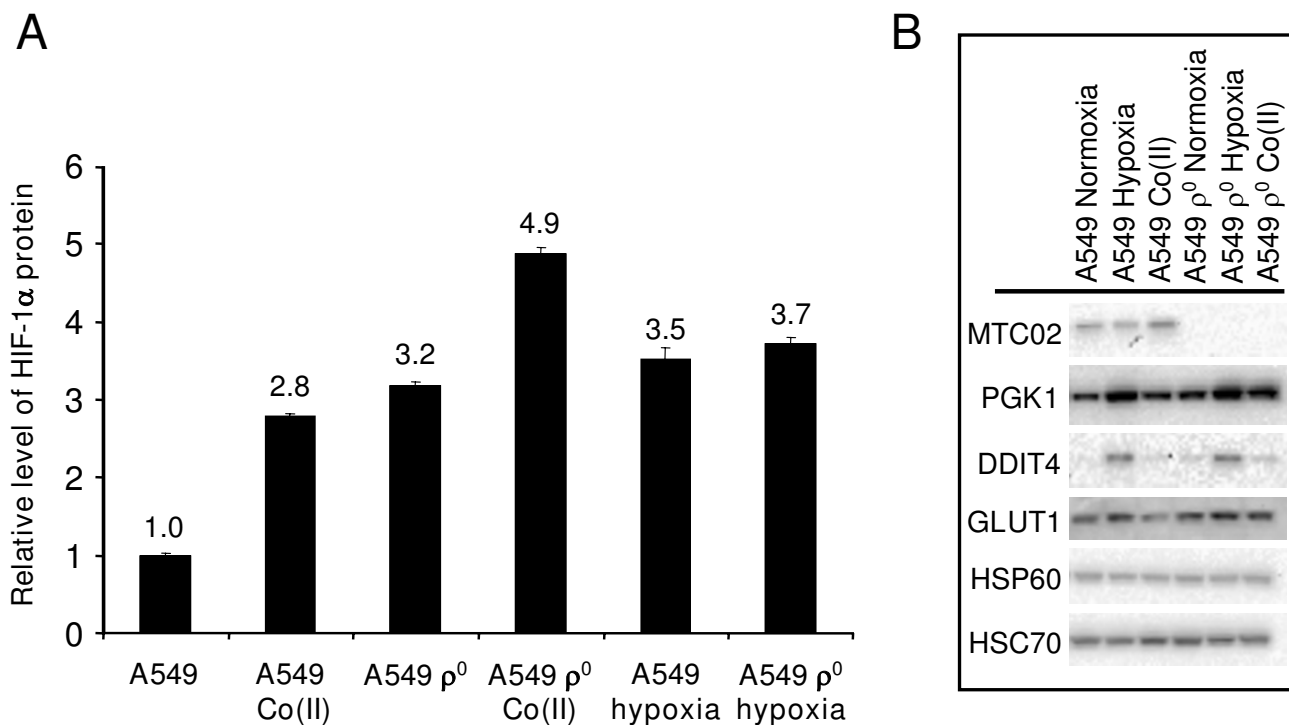
Figure 3
Levels of HIF-1α and HIF-1 target proteins in A549 and A549 ρ⁰ cells. Plateau phase cultures were treated with control vehicle (mannitol), cobalt acetate (cobalt, 100 μM), or hypoxia (1.5% oxygen atmosphere). (*A*) Levels of HIF-1α protein relative to control vehicle after 4 hours treatment as measured by ELISA. Effect of incubation under hypoxic conditions or with cobalt acetate is shown for comparison. Error bars indicate one standard deviation. (*B*) Representative Western blot showing MT-CO2, PGK1, DDIT4, GLUT1, and HSP60 levels in A549 and A549 ρ⁰ cells. PGK1 and DDIT4 levels were more abundant (1.4- and 4.0-fold, respectively) in A549 ρ⁰ cells relative to A549 cells. In contrast, GLUT1 and HSP60 levels were only marginally changed (1.1- and 1.25-fold less abundant) in A549 ρ⁰ cells relative to A549 cells. All estimates were made via phorphorimaging analysis with HSC70 levels serving as a loading control. Note that MT-CO2 levels could not be detected in any A549 ρ⁰ experiment while DDIT4 was expressed at low levels, but could be quantified in normoxic cells.

with the post-translational control of HIF-1 α activity (protein modification or subunit localization) and/or the activity of other transcription factors.

Contribution of mtDNA to gene expression profiles of cultured cells and xenografts

While gene expression differences between A549 cells grown in culture and in xenograft have been reported [59], comparison for both parental and mtDNA-deficient cells have not been previously performed. Interestingly, a greater number of transcripts were differentially expressed due to growth conditions (culture versus xenograft) than by mtDNA status. Importantly, infiltrating mouse cells have been demonstrated not to influence significantly gene expression profiles of tumor xenografts when using similar Affymetrix human microarrays [59]. All 2,512 transcripts that were differentially expressed in xenograft

versus culture for the parental A549 line are listed in Additional File 9. The 2,108 differentially expressed transcripts for the A549 ρ⁰ cells grown in xenograft versus culture are listed in Additional File 10 (see Additional File 3 for volcano plot). These results are borne out by hierarchical clustering analysis which first shows a clear separation of the gene expression profiles grown in culture versus xenograft and then separation according to mtDNA status, based on gene expression data obtained from 538 probe sets whose coefficient of variation was greater than 0.10 (Fig. 4).

We calculated the relative fraction of the variance associated with mtDNA status in the gene expression profiles from A549 ρ0 and parental A549 cells grown in culture and in xenografts (Additional File 2). In particular, we focused on those transcripts for which over 50% of the

variance (Benjamini and Hochberg corrected Bayes moderated F test P < 0.01) could be explained by mtDNA status and where there was significant differential expression in any two of the pair-wise comparisons of A549 ρ0 and parental A549 cells grown in culture or in xenograft. Overall, we discovered 430 transcripts (229 up-regulated and 201 down-regulated in A549 ρ0 relative to the parental A549 cells) that met these criteria (Additional File 11). Table 1 provides a listing of a subset of these transcripts where at least 90% of the variance in gene expression was dependent upon mtDNA status.

Importantly, the probe set that was most strongly affected (in this case down-regulated) by mtDNA status measures the relative abundance of *MT-ND5*, the only mtDNA-encoded transcript represented in this microarray (Table 1). *MT-ND5* is not expressed in the A549 ρ0 cells in culture or in xenograft (i.e. ranking within the lowest 15th percentile of all median gene expression scores in both cases). This provided us with empirical proof that our sorting strategy was sensitive to detecting transcripts dependent upon mtDNA status. Overall, we found that the variance in the expression of transcripts within MHC-1 (6 transcripts) and glucuronidation (4 transcripts) GO categories are all highly dependent upon mtDNA status (Fig. 5). These transcripts were more abundant in A549 ρ0 relative to the parental A549 cells. The MHC-1 and glucuronosyltransferase categories were previously discussed as having significance for the immune surveillance of cells with effective mitochondria and the detoxification of lipids that can accumulate due to defects in fatty acid metabolism. On the other hand, transcripts related to the protein complex assembly (11 transcripts) and chromatin (7 transcripts) GO categories were highly dependent upon mtDNA status and less abundant in A549 ρ0 cells relative to the parental A549 cells (Additional File 12). This could reflect their slower growth rates relative to the parental cell line.

In addition, mtDNA status affected multiple transcripts related to the above discussed epithelial-mesenchymal transition (EMT). Over 50% of the variance in the expression levels derived from probe sets for the previously described *SNAI2*, *ITGB3*, *CDH1*, and *FGA* genes could be explained by mtDNA status. The expression levels of all these genes indicated A549 ρ0 cells have increased mesenchymal phenotypes relative to the parental A549 cells. However, the fold-changes in expression of these genes in ρ0 versus parental cells were greater in culture than in the tumor xenografts (Additional File 2).

In contrast to genome-wide expression studies performed in yeast lacking mtDNA (ρ0 petites), we observed no evidence for a strong dependence of the variance in peroxisomal gene expression (especially based on 26 probe sets for peroxin (*PEX*) genes responsible for peroxisome assembly) due to mtDNA status [60]. Nevertheless, this does not preclude mtDNA status affecting peroxisome function, through abundance and/or activity. For example, we observed that the mtDNA status had a significant effect on *PHYH* expression (explains 76% of the observed variance in expression, F-test $P = 4.56 \times 10^{-4}$). *PHYH* encodes a peroxisomal enzyme critical for the catabolism of phytanic acid, a branched chain fatty acid [61,62]. *AMACR*, which also encodes an enzyme critical for phytanic acid metabolism, is also expressed higher in A549 ρ0 xenografts relative to A549 xenografts (2.0-fold, corrected *P* = 0.007). Interestingly, AMACR, which localizes to both peroxisomes and mitochondria, is an emerging biomarker for prostate cancer [63]. Given reports of frequent mitochondrial defects in prostate cancer [64], it is tempting to speculate that the over-expression of AMACR in prostate cancer could be related to defective mitochondrial function. However, it should be emphasized that the mitochondrial defects in our mtDNA-depleted A549 system will be more severe than those found in human tumors.

mtDNA-dependent expression profiles show agreement with prior reports

It can be questioned whether the observed mtDNA-dependent gene expression profiles are (i) shared amongst all cell lines, (ii) unique to our system, or (iii) reflect possible mutations in acquired in the nuclear genome of the ethidium bromide-treated A549 ρ0 cells. To begin to address these issues, we searched for previous reports of differential gene expression in cultured ρ0 cells relative to their parental cell lines. It is important to note that there is a limited literature on gene expression profiling in mtDNA-depleted cell cultures [16,44,65,66] and that there are no previous reports of gene expression profiling in mtDNA-depleted xenografts. Nevertheless, we found confirmatory evidence for our observed major categories of mtDNA-dependent transcripts levels including: tRNA synthetases (over-expressed in osteosarcoma ρ0 cells [66] and lymphoblastoid ρ0 cells [44]), MHC-related transcript (over-expressed in osteosarcoma ρ0 cells [56] and breast cancer ρ0 cells [65]), UDP-glucuronosyltransferase (over-expressed in breast cancer ρ0 cells [65]), and HIF1-α (over-expressed in lymphoblastoid ρ0 cells [44]). Furthermore, the *FXY2D2* (aka *ATP1G1*) and the *VLDR* transcripts, whose levels were strongly dependent upon mtDNA-status and over-abundant in A549 ρ0 cells (Table 1), were found to be over-expressed in human fibroblasts with mutations in nuclear-encoded mitochondrial Complex I genes [67] and retinal pigment epithelial ρ0 cells [14], respectively. Similarly, metallothionein transcripts were over-expressed in fibroblasts containing mutated nuclear-encoded mitochondrial genes, in agreement with our observations in A549 ρ0 cell cultures [67]. Thus, results from multiple laboratories testing different ρ0 cell

cultures support the assertion that our current analyses at least partially reflect mtDNA-dependent gene expression relevant to multiple cell types. Future gene expression profiling experiments of mtDNA-depleted cells generated using non-chemical-based protocols, such as expressing siRNA against the *TFAM* gene [68] or a dominant negative form of the mitochondria-specific DNA polymerase-gamma [69], could provide valuable empirical data to assess our candidate mtDNA-dependent gene expression profiles. Ultimately, large-scale proteomic characterization of mtDNA-depleted and parental cells will be necessary to rigorously assess possible functional consequences of differential gene expression [15,70].

Contribution of growth conditions to gene expression profiles

Next, we calculated the relative fraction of the variance associated with growth conditions in the gene expression profiles from ρ^0 and parental cells grown in culture and in xenografts. At first, we focused on those transcripts for which over 50% of the variance (corrected F test $P < 0.01$) could be explained by growth conditions and where there was differential expression in any of the pair-wise comparisons of ρ^0 and parental A549 cells grown in culture or in xenograft. Overall, we uncovered 2,633 transcripts that met these criteria. In order to reduce transcript complexity, we focused on the subset of 551 transcripts (316 up-regulated and 235 down-regulated in xenografts relative
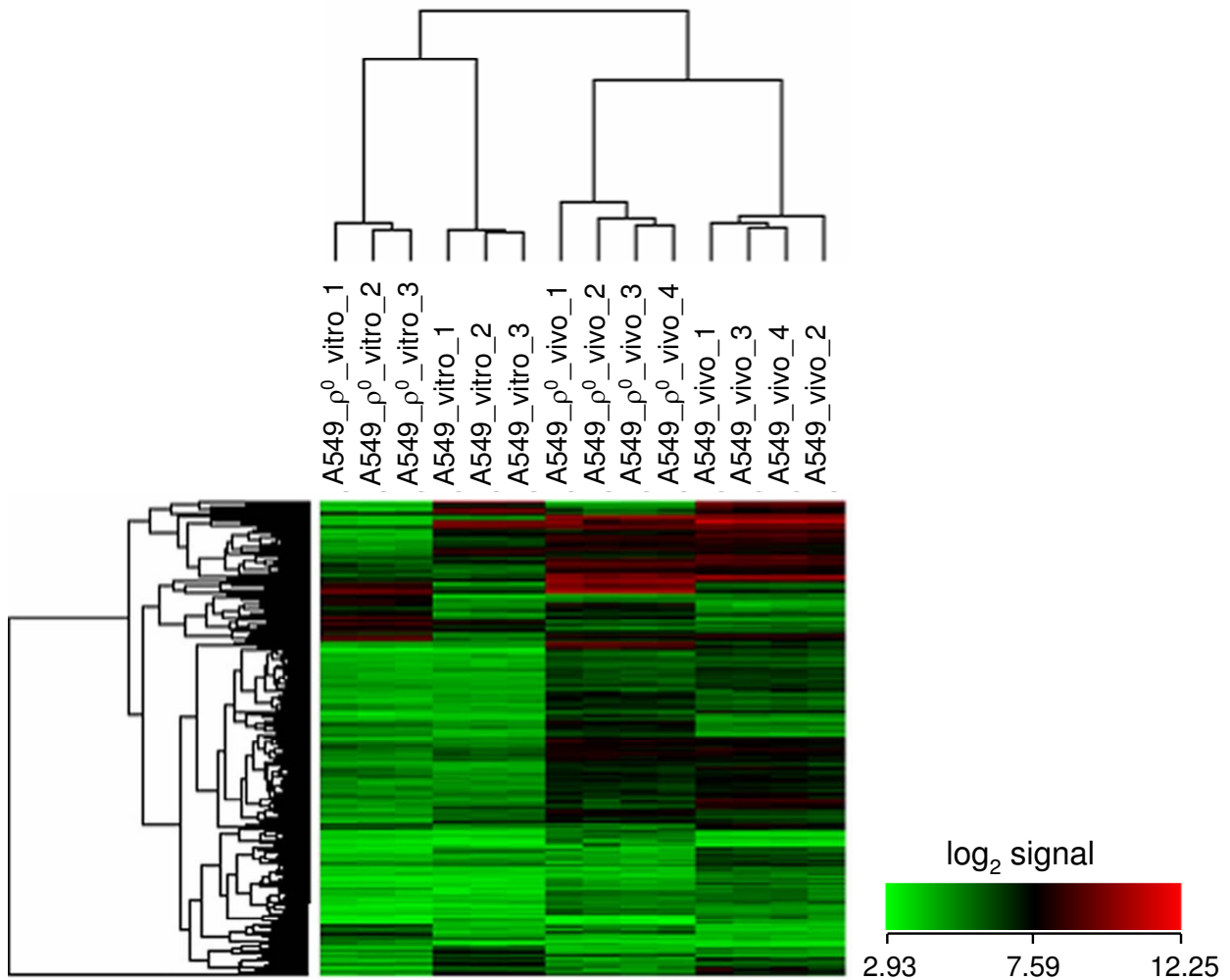

Figure 4
Hierarchical clustering analysis of expression data from A549 and A549 ρ^0 cells in culture and in xenografts. The dendrograms were generated based on average linkage hierarchical clustering of expression data from 538 probe sets whose coefficient of variation was greater than 0.10. Data from A549 cultures are provided in triplicate.

to cultured cells) where growth conditions contributed to a robust 90% of the variance observed in the data set (Additional File 13). Table 2 lists a subset of these transcripts where at least 97% of the variance in gene expression was dependent upon mtDNA status.

Of the GO categories enriched for transcripts whose expression was highly dependent upon growth conditions, only the nuclear RNA splicing GO category (9 tran-

scripts) were more abundant in xenografts relative to cultured cells (Additional File 14A). However, multiple GO categories were enriched for transcripts whose variance was principally explained by growth conditions and were less abundant in xenografts relative to cell culture. These included categories related to mitochondrial function (50 mitochondrion transcripts), glycolysis (7 transcripts), electron carrier activity (11 transcripts), purine
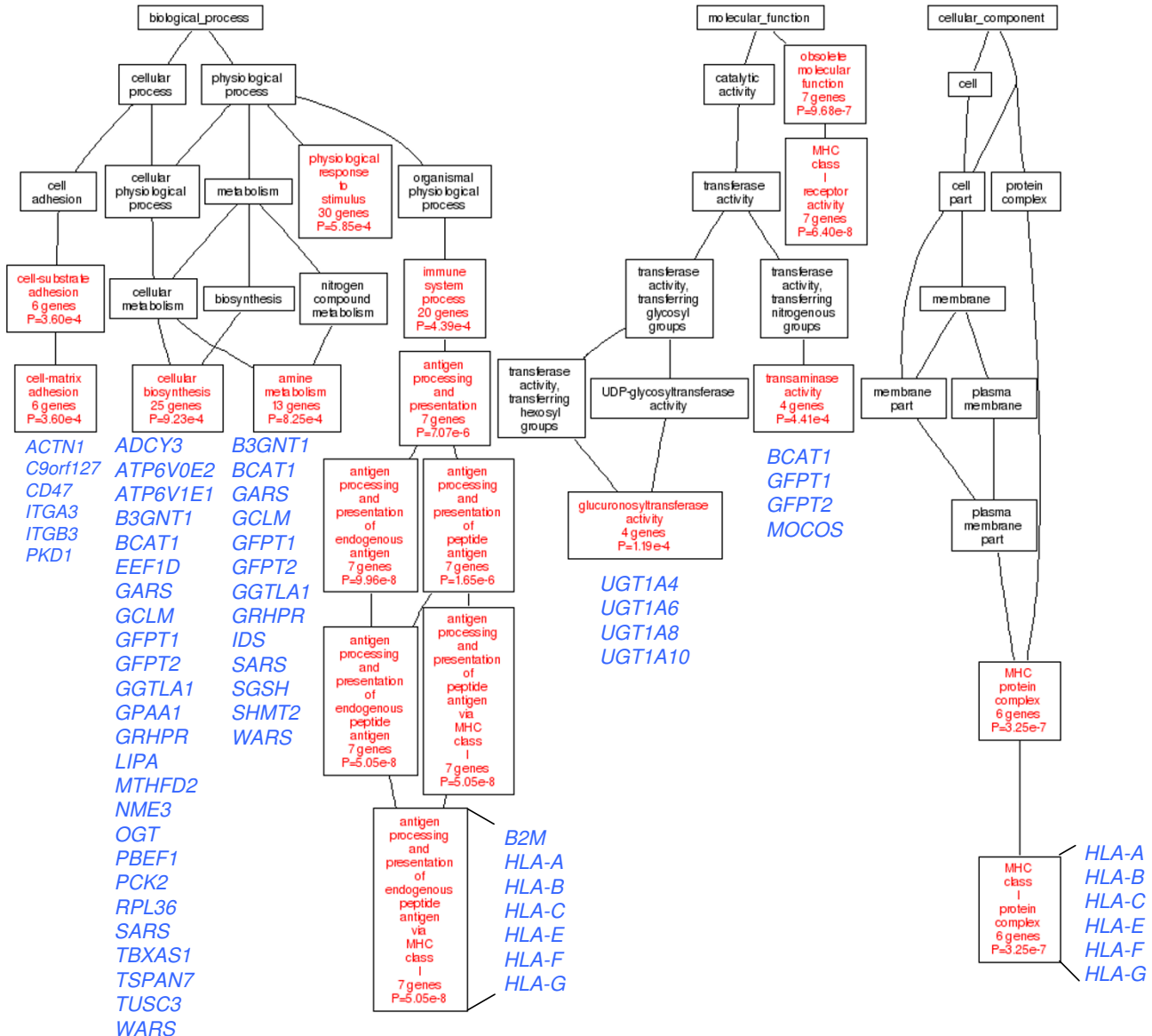

Figure 5
Gene Ontology analysis of up-regulated transcripts in ρ^0 cells whose variance is strongly influenced by mtDNA status. The directed acyclic graph (DAG) represents the relationships of categories (shown in red) that are enriched for transcripts where mtDNA status accounted for over 50% of the observed variance in gene expression and are more abundant *in vitro* (i.e. cell culture) and/or *in vivo* (i.e. xenograft) in A549 ρ^0 cells relative to parental A549 cells. All 229 probe sets used in this analysis are provided in Additional File 11. The names of genes in terminal categories are provided the blue.

Table 2: Transcripts where 97% of the variance in gene expression is explained by growth conditions

	Affymetrix Probe ID[a]	Gene Symbol	Entrez GeneID	Gene Description	Growth Prop. of Variance[b]	F test[c]	ρ^0 Vivo/ρ^0 Vitro		WT Vivo/WT Vivo	
							FC[d]	P[e]	FC[d]	P[e]
Up-regulated and dependent on growth conditions	211571_s_at	CSPG2	1462	chondroitin sulfate proteoglycan 2	0.99	1.41×10^{-12}	34.6	0.0001	19.0	0.0002
	215646_s_at	CSPG2	1462	chondroitin sulfate proteoglycan 2	0.99	2.52×10^{-12}	33.5	0.0003	20.3	0.0003
	220952_s_at	PLEKHA5	54477	PI 3-phosphate-binding protein-2	0.99	1.79×10^{-11}	6.7	0.0003	5.6	0.0006
	209090_s_at	SH3GLB1	51100	SH3-domain GRB2-like endophilin B1	0.99	2.86×10^{-10}	3.0	0.0015	3.1	0.0002
	216405_at	LGALS1	3956	lectin, galactoside-binding, soluble, 1	0.98	6.43×10^{-12}	11.5	0.0007	14.4	0.0006
	212254_s_at	DST	667	dystonin	0.98	3.64×10^{-11}	3.9	0.0006	4.7	0.0003
	201056_at	GOLGB1	2804	golgin B1, golgi integral mem. protein	0.98	2.12×10^{-10}	3.3	0.0008	2.9	0.0004
	221829_s_at	TNPO1	3842	transportin 1	0.98	2.86×10^{-10}	4.0	0.0012	3.9	0.0005
	204619_s_at	CSPG2	1462	chondroitin sulfate proteoglycan 2	0.98	3.01×10^{-11}	12.2	0.0003	7.5	0.0003
	205173_x_at	CD58	965	CD58 molecule	0.98	1.70×10^{-10}	3.5	0.0014	3.7	0.0004
	218901_at	PLSCR4	57088	phospholipid scramblase 4	0.98	1.32×10^{-9}	3.5	0.0009	3.8	0.0014
	213229_at	DICER1	23405	Dicer1, Dcr-1 homolog	0.97	2.18×10^{-10}	6.1	0.0009	7.0	0.0013
	208772_at	ANKHD1	404734	ankyrin repeat & KH domain containing 1	0.97	1.97×10^{-9}	2.5	0.0027	2.4	0.0003
	221731_x_at	CSPG2	1462	chondroitin sulfate proteoglycan 2	0.97	4.35×10^{-11}	104.7	0.0001	30.9	0.0002
	201057_s_at	GOLGB1	2804	golgin B1, golgi integral mem. protein	0.97	1.39×10^{-9}	3.2	0.0027	2.9	0.0002
	214295_at	KIAA0485	57235	KIAA0485 protein	0.97	4.14×10^{-10}	3.9	0.0014	4.1	0.0008
	201024_x_at	EIF5B	9669	eukaryotic translation initiation factor 5B	0.97	2.66×10^{-9}	2.3	0.0012	2.2	0.0012
	201280_s_at	DAB2	1601	disabled homolog 2	0.97	4.14×10^{-10}	5.3	0.0004	3.5	0.0006
	218396_at	VPS13C	54832	vacuolar protein sorting 13 homolog C	0.97	8.54×10^{-10}	4.4	0.0012	4.8	0.0006
	205383_s_at	ZBTB20	26137	zinc finger and BTB domain containing 20	0.97	5.52×10^{-10}	4.2	0.0011	6.7	0.0003
	219221_at	ZBTB38	253461	zinc finger and BTB domain containing 38	0.97	2.98×10^{-12}	6.0	0.0007	6.5	0.0003
	208663_s_at	TTC3	7267	tetratricopeptide repeat domain 3	0.97	1.19×10^{-9}	3.1	0.0021	3.1	0.0013
	212070_at	GPR56	9289	G protein-coupled receptor 56	0.97	3.78×10^{-10}	3.3	0.0007	4.3	0.0008
	203216_s_at	MYO6	4646	myosin VI	0.97	2.35×10^{-9}	3.1	0.0018	2.7	0.0012
	204620_s_at	CSPG2	1462	chondroitin sulfate proteoglycan 2	0.97	6.97×10^{-11}	104.5	0.0001	27.8	0.0002

Table 2: Transcripts where 97% of the variance in gene expression is explained by growth conditions *(Continued)*

	212062_at	ATP9A	10079	ATPase, Class II, type 9A	0.97	2.73×10^{-9}	2.5	0.0002	2.7	0.0030
	213775_x_at	ZNF638	27332	zinc finger protein 638	0.97	2.86×10^{-10}	2.6	0.0008	3.0	0.0005
Down-regulated and dependent on growth conditions	213201_s_at	TNNT1	7138	troponin T type 1	0.99	6.43×10^{-12}	-6.9	0.0002	-5.0	0.0003
	212432_at	GRPEL1	80273	GrpE-like 1, mitochondrial	0.99	1.37×10^{-9}	-2.3	0.0008	-2.3	0.0005
	209507_at	RPA3	6119	replication protein A3, 14 kDa	0.98	6.76×10^{-10}	-2.2	0.0010	-2.3	0.0002
	209825_s_at	UCK2	7371	uridine-cytidine kinase 2	0.98	1.09×10^{-9}	-2.5	0.0019	-2.3	0.0006
	202533_s_at	DHFR	1719	dihydrofolate reductase	0.98	3.51×10^{-9}	-2.1	0.0013	-2.0	0.0006
	201577_at	NME1	4830	non-metastatic cells 1, protein expressed	0.97	2.29×10^{-9}	-2.1	0.0014	-2.0	0.0004
	208756_at	EIF3S2	8668	euk. transl. init. factor 3, subunit 2 beta	0.97	1.92×10^{-8}	-1.8	0.0002	-1.7	0.0013
	207239_s_at	PCTK1	5127	PCTAIRE protein kinase 1	0.97	6.29×10^{-9}	-1.9	0.0017	-1.9	0.0007
	204126_s_at	CDC45L	8318	CDC45 cell division cycle 45-like	0.97	2.31×10^{-8}	-2.0	0.0030	-1.9	0.0004
	219162_s_at	MRPL11*	65003	mitochondrial ribosomal protein L11	0.97	1.37×10^{-9}	-2.5	0.0010	-2.2	0.0006
	208847_s_at	ADH5	128	alcohol dehydrogenase 5, chi polypeptide	0.97	5.92×10^{-8}	-1.7	0.0022	-1.6	0.0007
	210250_x_at	ADSL	158	adenylosuccinate lyase	0.97	4.04×10^{-9}	-2.0	0.0015	-2.3	0.0012
	208799_at	PSMB5	5693	proteasome beta 5 subunit	0.97	2.6×10^{-8}	-1.9	0.0025	-1.8	0.0004
	221620_s_at	NOMO3	408050	NODAL modulator 3	0.97	1.64×10^{-9}	-2.0	0.0015	-2.3	0.0004
	210519_s_at	NQO1	1728	NAD(P)H dehydrogenase, quinone 1	0.97	7.60×10^{-9}	-2.1	0.0020	-1.8	0.0007
	208910_s_at	C1QBP	708	splicing factor SF2-associated protein	0.97	1.63×10^{-9}	-2.4	0.0020	-2.5	0.0008
	201903_at	UQCRC1	7384	ubiquinol-cytochrome c reductase	0.97	9.25×10^{-9}	-1.8	0.0019	-2.1	0.0009
	200039_s_at	PSMB2	5690	proteasome subunit, beta type, 2	0.97	5.72×10^{-9}	-1.9	0.0022	-2.0	0.0006
	217960_s_at	TOMM22	56993	mitochondrial import receptor Tom22	0.97	1.04×10^{-8}	-2.2	0.0007	-1.9	0.0014
	205691_at	SYNGR3	9143	synaptogyrin 3	0.97	1.83×10^{-9}	-3.1	0.0012	-2.4	0.0012

[a]Only probe tilings representing genes with annotated functions are provided
[b]Proportion of variance in gene expression due to growth conditions (i.e. cultured cells or xenografts)
[c]Bayes modified F test (multiple hypothesis corrected)
[d]Fold-change [e]Benjamini and Hochberg corrected two-tailed Student's t-test

metabolism (5 transcripts), and the proteosome core complex (6 transcripts) (Additional File 14B).

The decrease in mitochondrial transcripts encoded by the nuclear genome may relate to the relative oxygen deprivation in xenografts relative to cell culture which would cause cells to rely less upon oxidative phosphorylation for their energy needs. The fact that growth conditions play a larger role in the expression of nuclear-encoded mitochondrial genes than the presence of the mitochondrial genome is not surprising if one considers the fact that ρ^0 cells form mitochondrial structures in the absence of mtDNA. Furthermore, this is consistent with observations that there are no differences in the expression of nuclear-encoded oxidative phosphorylation genes in parental and mtDNA-deficient osteosarcoma cells [71]. Interestingly, we could not detect differential transcript levels of nuclear encoded mtDNA polymerase (*POLG*), previously reported to be decreased on the protein level in HeLa ρ^0 cells [72], in any pair-wise comparison of experimental grouping performed in this study. However, we did find growth conditions accounted for 73% of the variance in gene expression (corrected F test $P = 8.3 \times 10^{-6}$ and down-regulated in xenografts) of the nuclear encoded mitochondrial RNA polymerase *POLRMT*, which was reported to be down-regulated on the protein level in response to mtDNA depletion in HeLa cells [72].

The above observations, also supported by KEGG (Kyoto Encyclopedia of Genes and Genomes) pathway analyses of the same group of transcripts (Additional File 15), indicate that both glycolysis and aerobic respiration-related genes are less abundant in xenografts relative to culture. This could relate to the cells being cultured in glucose-rich medium that does not reflect the situation found *in vivo*. In combination, decreased glycolysis and oxidative phosphorylation in xenografts reflects lower energetic demands *in vivo*. Likewise, the decreased abundance of transcripts related to purine metabolism in xenografts is likely related to slower growth rates in xenografts relative to culture. Decreased purine metabolism could also reflect the absence of the super-physiological levels of glutamine present in cell culture media.

Role of mtDNA mutations in human disorders
A549 lung cancer cells provide an appealing model system to study mitochondrial function due to their ability to be grown in culture and in tumor xenografts. The potential role of mitochondrial function in cancer was first recognized by Otto Warburg when he observed that cancer cells show a characteristic shift in energy production from oxidative phosphorylation to glycolysis [73]. More recently, there has been increasing appreciation of the possible importance of inherited and somatic mtDNA mutations in cancer [74]. Based on the gene expression

profiles observed in this study, ρ^0 xenograft tumor models could be of particular interest in determining mtDNA-mediated responses to specific cancer therapies, such anti-angiogenic agents.

In addition, ρ^0 cells play a critical role in the production of cybrid (cytoplasmic hybrid) cell lines containing specific mutations in mtDNA. While multiple groups have used this elegant system to study mitochondrial function in cultured cells (see reviews [4,75]), only recently have these cybrids been used in tumor xenografts [64]. Gene expression profiling of such cybrids both in culture and in xenografts could provide valuable data to elucidate further the functional interactions between the nuclear and mitochondrial genomes.

Conclusion
Although growth conditions had a greater influence on gene expression profiles than the presence of active mitochondria, we identified mtDNA-dependent gene expression profiles that are shared in cultured A549 cells and in xenografts. These profiles indicate that cells with mtDNA alterations have distinct biochemical properties that make them well-suited for elucidating responses to physiological perturbations, such as changes in oxygen and glucose levels, and testing the effects of specialized classes of chemotherapeutic agents. In addition, our studies suggest that gene expression profiling of mtDNA-depleted cells grown culture and in xenografts provide powerful means to investigate possible relationships between mitochondrial activity and gene expression profiles in normal and pathological cells.

Authors' contributions
JP carried out flow cytometry and immunoassays. PT and XM performed the xenograft studies. PL prepared mtDNA-depleted cells, performed oxygen consumption, flow cytometry, and ELISA assays, and participated in the design of the study. PKD performed gene expression profiling experiments and assisted in data analysis. KR performed mtDNA quantification studies. DMT and KDS analyzed gene expression data. DM and JH conceived of the study, interpreted the data, and wrote the manuscript.

Additional material

Additional file 1
Analysis of mitochondrial-encoded RNA transcript levels in A549 and A549 ρ0 xenografts by quantitative RT-PCR. Mitochondrial-encoded RNA transcript levels in A549 and A549 ρ0 xenografts are quantified by RT-PCR.
Click here for file
[http://www.biomedcentral.com/content/supplementary/1471-2164-9-521-S1.ppt]

Additional file 2

Processed gene expression scores for all microarray analyses. *Gene expression scores for all microarray experiments described in this manuscript.*
Click here for file
[http://www.biomedcentral.com/content/supplementary/1471-2164-9-521-S2.xls]

Additional file 3

Volcano plots for gene expression comparisons considered in this study. *The relationships between fold changes and P-values for the gene expression comparisons made in this study are provided.*
Click here for file
[http://www.biomedcentral.com/content/supplementary/1471-2164-9-521-S3.ppt]

Additional file 4

Differentially expressed transcripts in A549 ρ^0 and A549 cells grown in culture. *Probe sets showing differential expression in cultured A549 ρ^0 and A549 cells are provided.*
Click here for file
[http://www.biomedcentral.com/content/supplementary/1471-2164-9-521-S4.xls]

Additional file 5

Gene Ontology analysis of transcripts that are differentially expressed in A549 ρ^0 cells relative to parental A549 cells in culture. *Functional categories of transcripts showing differential expression in cultured A549 ρ^0 and A549 cells are provided.*
Click here for file
[http://www.biomedcentral.com/content/supplementary/1471-2164-9-521-S5.ppt]

Additional file 6

Analysis of HIF-1 responsive genes in A549 ρ^0 and A549 cells. *Gene expression profiles of HIF-1 responsive genes in A549 ρ^0 and A549 cells are provided.*
Click here for file
[http://www.biomedcentral.com/content/supplementary/1471-2164-9-521-S6.xls]

Additional file 7

Transcripts that are differentially expressed in A549 ρ^0 and A549 cells grown in xenografts. *Probe sets showing differential expression in A549 ρ^0 and A549 xenografts are provided.*
Click here for file
[http://www.biomedcentral.com/content/supplementary/1471-2164-9-521-S7.xls]

Additional file 8

Gene Ontology analysis of transcripts that are differentially expressed in A549 ρ^0 cells relative to parental A549 cells in xenografts. *Functional categories of transcripts showing differential expression in cultured A549 ρ^0 and A549 xenografts are provided.*
Click here for file
[http://www.biomedcentral.com/content/supplementary/1471-2164-9-521-S8.ppt]

Additional file 9

Differential expression in A549 xenografts and A549 cell cultures. *Probe sets showing differential expression in A549 xenografts and A549 cell cultures are provided.*
Click here for file
[http://www.biomedcentral.com/content/supplementary/1471-2164-9-521-S9.xls]

Additional file 10

Differential expression in A549 ρ^0 xenografts and A549 ρ^0 cell cultures. *Probe sets showing differential expression in A549 ρ^0 xenografts and A549 ρ^0 cell cultures are provided.*
Click here for file
[http://www.biomedcentral.com/content/supplementary/1471-2164-9-521-S10.xls]

Additional file 11

Probe sets where 50% or more of the variance in gene expression profiles is influenced by mtDNA status. *Probe sets where 50% or more of the variance in gene expression profiles is influenced by mtDNA status are provided.*
Click here for file
[http://www.biomedcentral.com/content/supplementary/1471-2164-9-521-S11.xls]

Additional file 12

Gene Ontology analysis of down-regulated transcripts in ρ^0 cells whose variance is strongly influenced by mtDNA status. *Functional categories of down-regulated transcripts in ρ^0 cells whose variance is strongly influenced by mtDNA status are provided.*
Click here for file
[http://www.biomedcentral.com/content/supplementary/1471-2164-9-521-S12.ppt]

Additional file 13

Probe sets where 90% or more of the variance in gene expression profiles is influenced by growth conditions. *Probe sets where 90% or more of the variance in gene expression profiles is influenced by growth conditions are provided.*
Click here for file
[http://www.biomedcentral.com/content/supplementary/1471-2164-9-521-S13.xls]

Additional file 14

Gene Ontology analysis of transcripts whose variance are strongly dependent upon growth conditions. *Functional categories of transcripts whose variance are strongly dependent upon growth conditions are provided.*
Click here for file
[http://www.biomedcentral.com/content/supplementary/1471-2164-9-521-S14.ppt]

Additional file 15

KEGG analysis of differentially expressed genes in A549 ρ^0 and A549 cells. *Biological pathways containing differentially expressed genes in A549 ρ^0 and A549 cells are provided.*
Click here for file
[http://www.biomedcentral.com/content/supplementary/1471-2164-9-521-S15.xls]

Acknowledgements

References

1. Singh KK: **Mitochondria damage checkpoint, aging, and cancer.** *Ann N Y Acad Sci* 2006, **1067:**182-190.
2. Scarlett DJ, Herst P, Tan A, Prata C, Berridge M: **Mitochondrial gene-knockout (rho0) cells: a versatile model for exploring the secrets of trans-plasma membrane electron transport.** *Biofactors* 2004, **20(4):**199-206.
3. Chandel NS, Schumacker PT: **Cells depleted of mitochondrial DNA (rho0) yield insight into physiological mechanisms.** *FEBS Lett* 1999, **454(3):**173-176.
4. Bacman SR, Moraes CT: **Transmitochondrial technology in animal cells.** *Methods Cell Biol* 2007, **80:**503-524.
5. Prokisch H, Andreoli C, Ahting U, Heiss K, Ruepp A, Scharfe C, Meitinger T: **MitoP2: the mitochondrial proteome database – now including mouse data.** *Nucleic Acids Res* 2006:D705-711.
6. Vo TD, Palsson BO: **Building the power house: recent advances in mitochondrial studies through proteomics and systems biology.** *Am J Physiol Cell Physiol* 2007, **292(1):**C164-177.
7. King M, Attardi G: **Human cells lacking mtDNA: repopulation with exogenous mitochondria by complementation.** *Science* 1989, **246(4929):**500-503.
8. King MP, Attardi G: **Isolation of human cell lines lacking mitochondrial DNA.** *Methods Enzymol* 1996, **264:**304-313.
9. Gilkerson RW, Margineantu DH, Capaldi RA, Selker JM: **Mitochondrial DNA depletion causes morphological changes in the mitochondrial reticulum of cultured human cells.** *FEBS Lett* 2000, **474(1):**1-4.
10. Arnould T, Mercy L, Houbion A, Vankoningsloo S, Renard P, Pascal T, Ninane N, Demazy C, Raes M: **mtCLIC is up-regulated and maintains a mitochondrial membrane potential in mtDNA-depleted L929 cells.** *FASEB J* 2003, **17(14):**2145-7.
11. Buchet K, Godinot C: **Functional F1-ATPase Essential in Maintaining Growth and Membrane Potential of Human Mitochondrial DNA-depleted rho ° Cells.** *J Biol Chem* 1998, **273(36):**22983-22989.
12. Amuthan G, Biswas G, Ananadatheerthavarada HK, Vijayasarathy C, Shephard HM, Avadhani NG: **Mitochondrial stress-induced calcium signaling, phenotypic changes and invasive behavior in human lung carcinoma A549 cells.** *Oncogene* 2002, **21(51):**7839-7849.
13. Amuthan G, Biswas G, Zhang S, Klein-Szanto A, Vijayasarathy C, Avadhani N: **Mitochondria-to-nucleus stress signaling induces phenotypic changes, tumor progression and cell invasion.** *EMBO J* 2001, **20(8):**1910-1920.
14. Miceli MV, Jazwinski SM: **Nuclear gene expression changes due to mitochondrial dysfunction in ARPE-19 cells: implications for age-related macular degeneration.** *Invest Ophthalmol Vis Sci* 2005, **46(5):**1765-1773.
15. Kulawiec M, Arnouk H, Desouki MM, Kazim L, Still I, Singh KK: **Proteomic analysis of mitochondria-to-nucleus retrograde response in human cancer.** *Cancer Biol Ther* 2006, **5(8):**967-975.
16. van Waveren C, Sun Y, Cheung HS, Moraes CT: **Oxidative phosphorylation dysfunction modulates expression of extracellular matrix – remodeling genes and invasion.** *Carcinogenesis* 2006, **27(3):**409-418.
17. Biswas G, Tang W, Sondheimer N, Guha M, Bansal S, Avadhani NG: **A distinctive physiological role for IkappaBbeta in the propagation of mitochondrial respiratory stress signaling.** *J Biol Chem* 2008, **283(18):**12586-12594.
18. Morais R, Zinkewich-Peotti K, Parent M, Wang H, Babai F, Zollinger M: **Tumor-forming Ability in Athymic Nude Mice of Human Cell Lines Devoid of Mitochondrial DNA.** *Cancer Res* 1994, **54(14):**3889-3896.
19. Yu M, Shi Y, Wei X, Yang Y, Zhou Y, Hao X, Zhang N, Niu R: **Depletion of mitochondrial DNA by ethidium bromide treatment inhibits the proliferation and tumorigenesis of T47D human breast cancer cells.** *Toxicol Lett* 2007, **170(1):**83-93.
20. Cavalli LR, Varella-Garcia M, Liang BC: **Diminished tumorigenic phenotype after depletion of mitochondrial DNA.** *Cell Growth Differ* 1997, **8(11):**1189-1198.
21. Swerdlow RH, Redpath GT, Binder DR, Davis JN 2nd, VandenBerg SR: **Mitochondrial DNA depletion analysis by pseudogene ratioing.** *J Neurosci Methods* 2006, **150(2):**265-271.
22. Herrnstadt C, Clevenger W, Ghosh SS, Anderson C, Fahy E, Miller S, Howell N, Davis RE: **A novel mitochondrial DNA-like sequence in the human nuclear genome.** *Genomics* 1999, **60(1):**67-77.
23. Papandreou I, Cairns R, Fontana L, Lim A, Denko N: **HIF-1 mediates adaptation to hypoxia by actively downregulating mitochondrial oxygen consumption.** *Cell Metab* 2006, **3(3):**187-197.
24. Wang Z, Lecane P, Thiemann P, Fan Q, Cortez C, Ma X, Tonev D, Miles D, Naumovski L, Miller R, *et al.*: **Synthesis and biologic properties of hydrophilic sapphyrins, a new class of tumor-selective inhibitors of gene expression.** *Molecular Cancer* 2007, **6(1):**9.
25. Magda D, Lecane P, Miller RA, Lepp C, Miles D, Mesfin M, Biaglow JE, Ho VV, Chawannakul D, Nagpal S, *et al.*: **Motexafin gadolinium disrupts zinc metabolism in human cancer cell lines.** *Cancer Res* 2005, **65(9):**3837-3845.
26. Smyth GK: **Linear models and empirical bayes methods for assessing differential expression in microarray experiments.** *Stat Appl Genet Mol Biol* 2004, **3:**.
27. Gentleman RC, Carey VJ, Bates DM, Bolstad B, Dettling M, Dudoit S, Ellis B, Gautier L, Ge Y, Gentry J, *et al.*: **Bioconductor: open software development for computational biology and bioinformatics.** *Genome Biol* 2004, **5(10):**R80.
28. Hochberg Y, Benjamini Y: **More powerful procedures for multiple significance testing.** *Stat Med* 1990, **9(7):**811-818.
29. Kirov SA, Zhang B, Snoddy JR: **Association analysis for large-scale gene set data.** *Methods Mol Biol* 2007, **408:**19-33.
30. Zhang B, Schmoyer D, Kirov S, Snoddy J: **GOTree Machine (GOTM): a web-based platform for interpreting sets of interesting genes using Gene Ontology hierarchies.** *BMC Bioinformatics* 2004, **5:**16.
31. Zhang B, Kirov S, Snoddy J: **WebGestalt: an integrated system for exploring gene sets in various biological contexts.** *Nucleic Acids Res* 2005:W741-748.
32. Sirotnak F, Zakowski M, Miller V, Scher H, Kris M: **Efficacy of cytotoxic agents against human tumor xenografts is markedly enhanced by coadministration of ZD1839 (Iressa), an inhibitor of EGFR tyrosine kinase.** *Clin Cancer Res* 2000, **6(12):**4885-4892.
33. Holmuhamedov E, Jahangir A, Bienengraeber M, Lewis LD, Terzic A: **Deletion of mtDNA disrupts mitochondrial function and structure, but not biogenesis.** *Mitochondrion* 2003, **3(1):**13-19.
34. Park WH, Han YW, Kim SH, Kim SZ: **An ROS generator, antimycin A, inhibits the growth of HeLa cells via apoptosis.** *J Cell Biochem* 2007, **102(1):**98-109.
35. Garber K: **Epithelial-to-mesenchymal transition is important to metastasis, but questions remain.** *J Natl Cancer Inst* 2008, **100(4):**232-233.
36. Peinado H, Portillo F, Cano A: **Switching on-off Snail: LOXL2 versus GSK3beta.** *Cell Cycle* 2005, **4(12):**1749-1752.
37. Tukey RH, Strassburg CP: **Human UDP-glucuronosyltransferases: metabolism, expression, and disease.** *Annu Rev Pharmacol Toxicol* 2000, **40:**581-616.
38. Harding D, Fournel-Gigleux S, Jackson MR, Burchell B: **Cloning and substrate specificity of a human phenol UDP-glucuronosyltransferase expressed in COS-7 cells.** *Proc Natl Acad Sci USA* 1988, **85(22):**8381-8385.
39. Strassburg CP, Manns MP, Tukey RH: **Expression of the UDP-glucuronosyltransferase 1A locus in human colon. Identification**

and characterization of the novel extrahepatic UGT1A8. *J Biol Chem* 1998, **273(15):**8719-8726.

40. Mojarrabi B, Mackenzie PI: **Characterization of two UDP glucuronosyltransferases that are predominantly expressed in human colon.** *Biochem Biophys Res Commun* 1998, **247(3):**704-709.

41. Turgeon D, Chouinard S, Belanger P, Picard S, Labbe JF, Borgeat P, Belanger A: **Glucuronidation of arachidonic and linoleic acid metabolites by human UDP-glucuronosyltransferases.** *J Lipid Res* 2003, **44(6):**1182-1191.

42. Jakobs BS, Bogert C van den, Dacremont G, Wanders RJ: **Beta-oxidation of fatty acids in cultured human skin fibroblasts devoid of the capacity for oxidative phosphorylation.** *Biochim Biophys Acta* 1994, **1211(1):**37-43.

43. Bell EL, Klimova T, Chandel NS: **Targeting the mitochondria for cancer therapy: regulation of hypoxia-inducible factor by mitochondria.** *Antioxid Redox Signal* 2008, **10(3):**635-640.

44. Behan Ai, Doyle S, Farrell M: **Adaptive responses to mitochondrial dysfunction in the [rho][degree sign] Namalwa cell.** *Mitochondrion* 2005, **5(3):**173-193.

45. Vaux EC, Metzen E, Yeates KM, Ratcliffe PJ: **Regulation of hypoxia-inducible factor is preserved in the absence of a functioning mitochondrial respiratory chain.** *Blood* 2001, **98(2):**296-302.

46. Semenza GL: **Oxygen-dependent regulation of mitochondrial respiration by hypoxia-inducible factor 1.** *Biochem J* 2007, **405(1):**1-9.

47. Eng C, Kiuru M, Fernandez MJ, Aaltonen LA: **A role for mitochondrial enzymes in inherited neoplasia and beyond.** *Nat Rev Cancer* 2003, **3(3):**193-202.

48. Carroll VA, Ashcroft M: **Role of Hypoxia-Inducible Factor (HIF)-1{alpha} versus HIF-2{alpha} in the Regulation of HIF Target Genes in Response to Hypoxia, Insulin-Like Growth Factor-I, or Loss of von Hippel-Lindau Function: Implications for Targeting the HIF Pathway.** *Cancer Res* 2006, **66(12):**6264-6270.

49. Stolze IP, Tian Y-M, Appelhoff RJ, Turley H, Wykoff CC, Gleadle JM, Ratcliffe PJ: **Genetic Analysis of the Role of the Asparaginyl Hydroxylase Factor Inhibiting Hypoxia-inducible Factor (HIF) in Regulating HIF Transcriptional Target Genes.** *J Biol Chem* 2004, **279(41):**42719-42725.

50. Duarte A, Castillo AF, Castilla R, Maloberti P, Paz C, Podesta EJ, Cornejo Maciel F: **An arachidonic acid generation/export system involved in the regulation of cholesterol transport in mitochondria of steroidogenic cells.** *FEBS Lett* 2007, **581(21):**4023-4028.

51. Di Paola M, Lorusso M: **Interaction of free fatty acids with mitochondria: coupling, uncoupling and permeability transition.** *Biochim Biophys Acta* 2006, **1757(9–10):**1330-1337.

52. Kumemura H, Harada M, Yanagimoto C, Koga H, Kawaguchi T, Hanada S, Taniguchi E, Ueno T, Sata M: **Mutation in keratin 18 induces mitochondrial fragmentation in liver-derived epithelial cells.** *Biochem Biophys Res Commun* 2008, **367(1):**33-40.

53. Tang HL, Lung HL, Wu KC, Le AH, Tang HM, Fung MC: **Vimentin supports mitochondrial morphology and organization.** *Biochem J* 2008, **410(1):**141-146.

54. Park SG, Ewalt KL, Kim S: **Functional expansion of aminoacyl-tRNA synthetases and their interacting factors: new perspectives on housekeepers.** *Trends Biochem Sci* 2005, **30(10):**569-574.

55. Tzima E, Schimmel P: **Inhibition of tumor angiogenesis by a natural fragment of a tRNA synthetase.** *Trends Biochem Sci* 2006, **31(1):**7-10.

56. Gu Y, Wang C, Roifman CM, Cohen A: **Role of MHC class I in immune surveillance of mitochondrial DNA integrity.** *J Immunol* 2003, **170(7):**3603-3607.

57. Kurz T, Terman A, Gustafsson B, Brunk UT: **Lysosomes and oxidative stress in aging and apoptosis.** *Biochim Biophys Acta* 2008.

58. Miceli MV, Jazwinski SM: **Common and cell type-specific responses of human cells to mitochondrial dysfunction.** *Exp Cell Res* 2005, **302(2):**270-280.

59. Creighton CJ, Bromberg-White JL, Misek DE, Monsma DJ, Brichory F, Kuick R, Giordano TJ, Gao W, Omenn GS, Webb CP, *et al.*: **Analysis of Tumor-Host Interactions by Gene Expression Profiling of Lung Adenocarcinoma Xenografts Identifies Genes Involved in Tumor Formation.** *Mol Cancer Res* 2005, **3(3):**119-129.

60. Epstein CB, Waddle JA, Hale Wt, Dave V, Thornton J, Macatee TL, Garner HR, Butow RA: **Genome-wide responses to mitochondrial dysfunction.** *Mol Biol Cell* 2001, **12(2):**297-308.

61. Jansen GA, Ofman R, Ferdinandusse S, Ijlst L, Muijsers AO, Skjeldal OH, Stokke O, Jakobs C, Besley GT, Wraith JE, *et al.*: **Refsum disease is caused by mutations in the phytanoyl-CoA hydroxylase gene.** *Nat Genet* 1997, **17(2):**190-193.

62. Mihalik SJ, Morrell JC, Kim D, Sacksteder KA, Watkins PA, Gould SJ: **Identification of PAHX, a Refsum disease gene.** *Nat Genet* 1997, **17(2):**185-189.

63. Adley BP, Yang XJ: **Application of alpha-methylacyl coenzyme A racemase immunohistochemistry in the diagnosis of prostate cancer: a review.** *Anal Quant Cytol Histol* 2006, **28(1):**1-13.

64. Petros JA, Baumann AK, Ruiz-Pesini E, Amin MB, Sun CQ, Hall J, Lim S, Issa MM, Flanders WD, Hosseini SH, *et al.*: **mtDNA mutations increase tumorigenicity in prostate cancer.** *Proc Natl Acad Sci USA* 2005, **102(3):**719-724.

65. Delsite R, Kachhap S, Anbazhagan R, Gabrielson E, Singh KK: **Nuclear genes involved in mitochondria-to-nucleus communication in breast cancer cells.** *Mol Cancer* 2002, **1:**6.

66. Jahangir Tafrechi RS, Svensson PJ, Janssen GM, Szuhai K, Maassen JA, Raap AK: **Distinct nuclear gene expression profiles in cells with mtDNA depletion and homoplasmic A3243G mutation.** *Mutat Res* 2005, **578(1–2):**43-52.

67. Westhuizen FH van der, Heuvel LP van den, Smeets R, Veltman JA, Pfundt R, van Kessel AG, Ursing BM, Smeitink JA: **Human mitochondrial complex I deficiency: investigating transcriptional responses by microarray.** *Neuropediatrics* 2003, **34(1):**14-22.

68. Jeng JY, Yeh TS, Lee JW, Lin SH, Fong TH, Hsieh RH: **Maintenance of mitochondrial DNA copy number and expression are essential for preservation of mitochondrial function and cell growth.** *J Cell Biochem* 2008, **103(2):**347-357.

69. Jazayeri M, Andreyev A, Will Y, Ward M, Anderson CM, Clevenger W: **Inducible expression of a dominant negative DNA polymerase-gamma depletes mitochondrial DNA and produces a rho0 phenotype.** *J Biol Chem* 2003, **278(11):**9823-9830.

70. Chevallet M, Lescuyer P, Diemer H, van Dorsselaer A, Leize-Wagner E, Rabilloud T: **Alterations of the mitochondrial proteome caused by the absence of mitochondrial DNA: A proteomic view.** *Electrophoresis* 2006, **27(8):**1574-1583.

71. Duborjal H, Beugnot R, De Camaret BM, Issartel JP: **Large functional range of steady-state levels of nuclear and mitochondrial transcripts coding for the subunits of the human mitochondrial OXPHOS system.** *Genome Res* 2002, **12(12):**1901-1909.

72. Seidel-Rogol BL, Shadel GS: **Modulation of mitochondrial transcription in response to mtDNA depletion and repletion in HeLa cells.** *Nucleic Acids Res* 2002, **30(9):**1929-1934.

73. Warburg O: **On the origin of cancer cells.** *Science* 1956, **123(3191):**309-314.

74. Brandon M, Baldi P, Wallace DC: **Mitochondrial mutations in cancer.** *Oncogene* 2006, **25(34):**4647-4662.

75. Swerdlow RH: **Mitochondria in cybrids containing mtDNA from persons with mitochondriopathies.** *J Neurosci Res* 2007, **85(15):**3416-3428.